Photosynthetic-Product–Dependent Activation of Plasma Membrane H$^+$-ATPase and Nitrate Uptake in *Arabidopsis* Leaves

Satoru N. Kinoshita[1], Takamasa Suzuki[2], Takatoshi Kiba[3], Hitoshi Sakakibara[3] and Toshinori Kinoshita[1,4,*]

[1]Graduate School of Science, Nagoya University, Chikusa, Nagoya, 464-8602 Japan
[2]Department of Biological Chemistry, College of Bioscience and Biotechnology, Chubu University, Kasugai, 487-8501 Japan
[3]Graduate School of Bioagricultural Sciences, Nagoya University, Nagoya, 464-8602 Japan
[4]Institute of Transformative Bio-Molecules (WPI-ITbM), Nagoya University, Chikusa, Nagoya, 464-8602 Japan

*Corresponding author: E-mail, kinoshita@bio.nagoya-u.ac.jp

Plasma membrane (PM) proton-translocating adenosine triphosphatase (H$^+$-ATPase) is a pivotal enzyme for plant growth and development that acts as a primary transporter and is activated by phosphorylation of the penultimate residue, threonine, at the C-terminus. Small Auxin-Up RNA family proteins maintain the phosphorylation level via inhibiting dephosphorylation of the residue by protein phosphatase 2C-D clade. Photosynthetically active radiation activates PM H$^+$-ATPase via phosphorylation in mesophyll cells of *Arabidopsis thaliana*, and phosphorylation of PM H$^+$-ATPase depends on photosynthesis and photosynthesis-related sugar supplementation, such as sucrose, fructose and glucose. However, the molecular mechanism and physiological role of photosynthesis-dependent PM H$^+$-ATPase activation are still unknown. Analysis using sugar analogs, such as palatinose, turanose and 2-deoxy glucose, revealed that sucrose metabolites and products of glycolysis such as pyruvate induce phosphorylation of PM H$^+$-ATPase. Transcriptome analysis showed that the novel isoform of the *Small Auxin-Up RNA* genes, *SAUR30*, is upregulated in a light- and sucrose-dependent manner. Time-course analyses of sucrose supplementation showed that the phosphorylation level of PM H$^+$-ATPase increased within 10 min, but the expression level of *SAUR30* increased later than 10 min. The results suggest that two temporal regulations may participate in the regulation of PM H$^+$-ATPase. Interestingly, a $^{15}NO_3^-$ uptake assay in leaves showed that light increases $^{15}NO_3^-$ uptake and that increment of $^{15}NO_3^-$ uptake depends on PM H$^+$-ATPase activity. The results opened the possibility of the physiological role of photosynthesis-dependent PM H$^+$-ATPase activation in the uptake of NO_3^-. We speculate that PM H$^+$-ATPase may connect photosynthesis and nitrogen metabolism in leaves.

Keywords: *Arabidopsis thaliana* ● C–N interaction ● Nitrate uptake ● Photosynthesis ● PM H$^+$-ATPase

Introduction

Photosynthesis in plants converts CO_2 and light energy into carbon (C) metabolites for translocation and energy production and is important for plant growth and reproduction. To maintain high photosynthetic activity, several inorganic elements are essential, such as nitrogen (N), potassium, magnesium and phosphorus (Tränkner et al. 2018, Evans and Clarke 2019). The N content of leaves is of utmost importance for photosynthetic capacity. Most of the N content in C$_3$ sun leaves is allocated to photosynthesis-related proteins such as light-harvesting complex, Rubisco and enzymes in the Calvin–Benson cycle (Evans and Clarke 2019). It is thus essential to maintain high N availability in leaves for active photosynthesis. To this end, vascular plants must uptake nitrate or other N metabolites from soil and translocate N to leaves in the form of nitrate or amino acids (Delhon et al. 1996, Matt et al. 2001).

Uptake of N—including nitrate, ammonium and amino acids—requires transport across the plasma membrane (PM). Therefore, N uptake is mediated by PM-localized transporters and channels. Among the N transporters and channels, nitrate transporters (NRTs) have been well characterized in a range of plant species, and most NRTs, such as the NRT1 and NRT2 families, are H$^+$-symporters (Hachiya and Sakakibara 2017). The association of the H$^+$ gradient across the PM with nitrate uptake by NRTs and another N uptake in roots has been investigated in several plant and crop species (Tong et al. 2005, Lupini et al. 2018, Zhang et al. 2021a). The association of the H$^+$ gradient across the PM with nitrate uptake in leaves of *Arabidopsis*

and cucumber has been suggested (Cookson et al. 2005, Nikolic et al. 2012).

The H$^+$ gradient and membrane potential across PM are maintained and polarized by H$^+$ extrusion from the cell, which is mediated by active P-type H$^+$ pumps, primarily PM proton-translocating adenosine triphosphatase (H$^+$-ATPase) (EC. 7.1.2.1) driven by ATP hydrolysis (Sondergaard et al. 2004). The physiological role of PM H$^+$-ATPase in plants is not limited to nutrient uptake, also encompassing dormancy alleviation in seeds (de Bont et al. 2019), cell elongation in hypocotyl (Takahashi et al. 2012), stomatal opening in guard cells (Assmann et al. 1985, Kinoshita and Shimazaki 1999), sugar loading in phloem (DeWitt and Sussman 1995) and pollen tube growth in flower pollen (Robertson et al. 2004, Hoffmann et al. 2020). *Arabidopsis* PM H$^+$-ATPase family consists of 11 genes. *AHA1* (AT2G18960) and *AHA2* (AT4G30190) are the two major isoforms in most of tissues, except for *AHA3* (AT5G57350) being major in phloem companion cells (DeWitt and Sussman 1995, Haruta et al. 2010). Double mutation of the two major isoforms of PM H$^+$-ATPase (*aha1 aha2*) in *Arabidopsis thaliana* leads to embryo death (Haruta et al. 2010), indicating that elucidation of its function in tissues using the double mutant is difficult. The H$^+$ pump activity of PM H$^+$-ATPase is regulated not only by its abundance but also by posttranslational modification (PTM) (Falhof et al. 2016). One of the major PTM regulators is phosphorylation of the penultimate residue, threonine (Thr), at the C-terminus, corresponding to Thr948 of AHA1 and Thr947 of AHA2. Phosphorylation of the penultimate Thr, simultaneous with 14-3-3 protein binding to the region, activates H$^+$ pumping (Palmgren 2001). Therefore, regulation of penultimate Thr phosphorylation by specific protein kinases and protein phosphatases determines the activity of PM H$^+$-ATPase in plants.

The signaling and regulatory mechanisms of PM H$^+$-ATPase have been identified. Phytohormones such as auxin and brassinosteroid induce phosphorylation of PM H$^+$-ATPase via the Small Auxin-Up RNAs (SAURs)–protein phosphatase 2C-D clade (PP2C-D) module in the hypocotyl of seedlings, resulting in cell elongation. Some of *SAUR* family genes, *SAUR19* (AT5G18010) and *SAUR63* (AT1G29440), are induced by exogenous auxin supplementation in seedling, and the SAUR proteins directly bind to the PP2C-D. Binding of SAURs to PP2C-D inhibits the dephosphorylation of penultimate Thr of PM H$^+$-ATPase by PP2C-D, thereby maintaining the high phosphorylated status of PM H$^+$-ATPase (Chae et al. 2012, Takahashi et al. 2012, Spartz et al. 2014, Ren et al. 2018, Minami et al. 2019, Wong et al. 2019). In guard cells, blue-light illumination induces phosphorylation of PM H$^+$-ATPase via phototropin-blue light signaling 1-blue light-dependent H$^+$-ATPase phosphorylation modules, leading to opening of stomata (Inoue and Kinoshita 2017). Recently, several SAURs–PP2C-D modules have been implicated in PM H$^+$-ATPase activation in guard cells (Wong et al. 2021, Akiyama et al. 2022). However, the activation mechanism of PM H$^+$-ATPase in photosynthetic tissues is unclear.

We have reported that photosynthetically active radiation of thalli of *Marchantia polymorpha*, protonemata of *Physcomitrella patens* or leaves of vascular plants induced phosphorylation of PM H$^+$-ATPase (Okumura et al. 2012a, 2012b, 2016, Harada et al. 2020). Although the mechanism is dependent on photosynthesis and its products (Okumura et al. 2016), the molecular mechanism and physiological role of PM H$^+$-ATPase activation in photosynthetic tissues are unknown.

Here, we characterized the molecular mechanism of photosynthesis-dependent phosphorylation of the penultimate Thr of PM H$^+$-ATPase and the physiological role of activated PM H$^+$-ATPase in *Arabidopsis* leaves. First, sugar-analog supplementation to leaves showed that the phosphorylation of PM H$^+$-ATPase is induced by glycolysis and the downstream metabolites. Second, a transcriptome analysis and time-course experiment implicated two temporal regulatory mechanisms in the phosphorylation of PM H$^+$-ATPase. Finally, isotope-labeled nitrate uptake assays implied that PM H$^+$-ATPase activation by photosynthesis may have a positive role in nitrate uptake in leaves. Therefore, our results propose that photosynthesis and the products activate the PM H$^+$-ATPase to compensate the N content in mesophyll cells.

Results

Involvement of glycolysis and the downstream in PM H$^+$-ATPase phosphorylation in leaves

Light-induced phosphorylation of the penultimate residue, Thr, of PM H$^+$-ATPase, which is required for PM H$^+$-ATPase activation, is likely mediated by endogenous photosynthetic products such as sucrose, glucose, fructose and organic acids in mesophyll cells of *A. thaliana* (Okumura et al. 2016, **Supplementary Fig. S1**). Because these activating metabolites are involved in sugar signaling such as sucrose and hexose signaling (Li and Sheen 2016), we used sugar analogs to assess whether phosphorylation of PM H$^+$-ATPase is dependent on some types of sugar signaling.

First, the effects of exogenous sucrose and the sucrose analogs, palatinose and turanose, were investigated. Palatinose and turanose are not metabolized in plants but induce the sucrose-specific signaling pathway (Fernie et al. 2001, Sinha et al. 2002). Palatinose, turanose, sucrose and mannitol were exogenously supplemented to pieces of leaves from overnight dark-adapted *Arabidopsis* in the dark. The effects of sugars on the phosphorylation level of the penultimate Thr of PM H$^+$-ATPase were determined using an antibody against the phosphorylated penultimate Thr of PM H$^+$-ATPase (anti-pThr; Hayashi et al. 2010). Palatinose and turanose had no effect on the phosphorylation level of PM H$^+$-ATPase, whereas sucrose induced PM H$^+$-ATPase phosphorylation (**Fig. 1A, B**), implying that PM H$^+$-ATPase phosphorylation is independent of the sucrose-specific signaling pathway but requires sucrose metabolism.

Second, 2-deoxy glucose (2DG) was used to investigate whether the phosphorylation of PM H$^+$-ATPase requires hexose phosphate accumulation and hexose signaling. 2DG is phosphorylated by hexokinases in cell but is not converted into fructose-6-phosphate; thus, 2DG phosphate accumulates intracellularly as hexose phosphate (Klein and Stitt 1998, Li and Sheen 2016). In addition, 2DG inhibits C flux to the glycolysis pathway in animal and plant species (Xiong et al. 2013, Pajak et al. 2020). Preincubation of 2DG alone and with mannitol did not alter the phosphorylation level of PM H$^+$-ATPase compared to the control [water (H$_2$O) alone], indicating that hexose phosphate accumulation or hexose signaling is not involved in the pathway (**Fig. 1C, D**). In addition, preincubation with 2DG significantly suppressed sucrose-induced phosphorylation of PM H$^+$-ATPase. Surprisingly, supplementation of pyruvate, the final product of glycolysis, induced phosphorylation of PM H$^+$-ATPase (**Fig. 1C, D**). Considering 2DG inhibits the C flow to glycolysis, these results imply that the metabolites of glycolysis and the downstream may be important in sucrose-induced phosphorylation of PM H$^+$-ATPase (**Fig. 1E**). The 2DG pretreatment partially affected pyruvate-induced phosphorylation of PM H$^+$-ATPase, but not significantly (**Fig. 1C, D**).

An activation mechanism of PM H$^+$-ATPase via the change of SAUR30 transcript level

To unravel the molecular mechanism by which photosynthesis controls phosphorylation of PM H$^+$-ATPase, the involvement of *SAUR* family genes was investigated. SAUR proteins activate PM H$^+$-ATPase by inhibiting PP2C-D family proteins, which directly dephosphorylate penultimate Thr of PM H$^+$-ATPase, in the hypocotyl of seedlings (Spartz et al. 2014, Ren et al. 2018, Wong et al. 2019). For this purpose, RNA-sequencing (RNA-seq) was performed to assess the expression levels of 79 *SAUR* family genes using overnight dark-adapted *Arabidopsis* leaves subjected to white-light illumination (Lt), or incubation with 30 mM sucrose solution (Suc) for 30 min. Reference control samples for the Lt and Suc conditions were overnight dark-adapted leaves (Dk) and 30 mM mannitol solution–incubated leaves (Man), respectively.

Eighteen *SAUR* family genes were identified as differentially expressed genes (DEGs; false discovery rate (FDR) < 0.05, fold change > 2) for the Lt/Dk comparison and four *SAUR* family genes for the Suc/Man comparison (**Fig. 2**). Only *SAUR30* (AT5G53590) was differentially expressed in both Lt and Suc with relatively high transcript per million (TPM) values (**Fig. 2**). The expression of *SAUR30* was increased 3.9-fold in the Lt/Dk comparison and 2.3-fold in the Suc/Man comparison. Other than *SAUR* genes, 2,663 DEGs were detected in the Lt/Dk comparison, and 367 in the Suc/Man comparison (**Supplementary Fig. S2A, Supplementary Data File S1**).

Additionally, 23% (62/270) of DEGs under both conditions overlapped with KIN10-dependent reference DEGs (Baena-González et al. 2007) (**Supplementary Fig. S2A**). KIN10 is a kinase subunit of SnRK1, a hub regulator of energy starvation. The overlapping genes showed reversed expression

changes compared to those caused by KIN10 overexpression (Baena-González et al. 2007) (**Supplementary Fig. S2B**), indicating that the leaf samples in our experiment were experiencing energy starvation after dark adaptation and energy recovery under light illumination and with exogenous sucrose supplementation (**Supplementary Fig. S2C**).

Next, to confirm the function of SAUR30 in PM H$^+$-ATPase phosphorylation in vivo, *SAUR30*-containing plasmids were transfected into mesophyll cell protoplasts (MCPs) using the polyethylene glycol (PEG)–Ca^{2+} method, and phosphorylation of endogenous PM H$^+$-ATPase in MCPs was examined. As expected, transiently expressed SAUR30 and SAUR30-green fluorescent proteins (GFPs) increased the phosphorylation level of PM H$^+$-ATPase in MCPs, whereas GFP alone and the no-protein-expression control (N.C.) did not (**Fig. 3, Supplementary Fig. S3**). We further confirmed that the high phosphorylation level of PM H$^+$-ATPase in SAUR30-expressed MCPs was decreased when co-expressed with mutated PP2C-Ds (**Supplementary Fig. S5**). These results indicate that the novel isoform of *SAUR*, *SAUR30*, may maintain PM H$^+$-ATPase phosphorylation in MCPs via the well-known SAUR-PP2C-D module model.

Earlier regulatory mechanisms of PM H$^+$-ATPase phosphorylation

The light-dependent phosphorylation of PM H$^+$-ATPase starts 15 min after Lt (Okumura et al. 2016). The quick response of PM H$^+$-ATPase to photosynthesis implies that phosphorylation of PM H$^+$-ATPase is not only regulated by the change of transcript level in leaves. To examine the temporal pattern of PM H$^+$-ATPase phosphorylation level and *SAUR30* transcript level in sucrose supplementation, pieces of leaves infiltrated with sucrose solution were sampled at 0, 2.5, 5.0, 10, 30 and 60 min after infiltration. Next, the phosphorylation level of PM H$^+$-ATPase and the expression level of *SAUR30* were evaluated by immunoblotting and real-time (RT)-quantitative polymerase chain reaction (PCR), respectively. Interestingly, PM H$^+$-ATPase phosphorylation was induced at around 5–10 min (**Fig. 4A, B**), while the *SAUR30* expression was induced markedly at 30 min after sucrose infiltration (**Fig. 4C**). These results implicate another regulatory mechanism (5–10 min; early response) in phosphorylation of PM H$^+$-ATPase in leaves.

To confirm the physiological function of SAUR30 protein in the temporal regulation, SAUR30-GFP overexpression plants under cauliflower mosaic virus 35S promoter (SAUR30-GFP OE) were generated. In line with SAUR19 and SAUR63 overexpression seedlings, the hypocotyl length of SAUR30-GFP OE seedlings was increased (Spartz et al. 2012, Chae et al. 2012, **Supplementary Fig. S6A**). The phosphorylation level of PM H$^+$-ATPase in illuminated leaves and seedling shoots was higher than the wild type (**Fig. 5A, C, Supplementary Fig. S6B**). The phosphorylation level of PM H$^+$-ATPase in sucrose-supplemented leaves of SAUR30-GFP OE was significantly higher after 2.5 min compared to that of the wild type (**Fig. 5B, D**), indicating that the SAUR30-GFP can
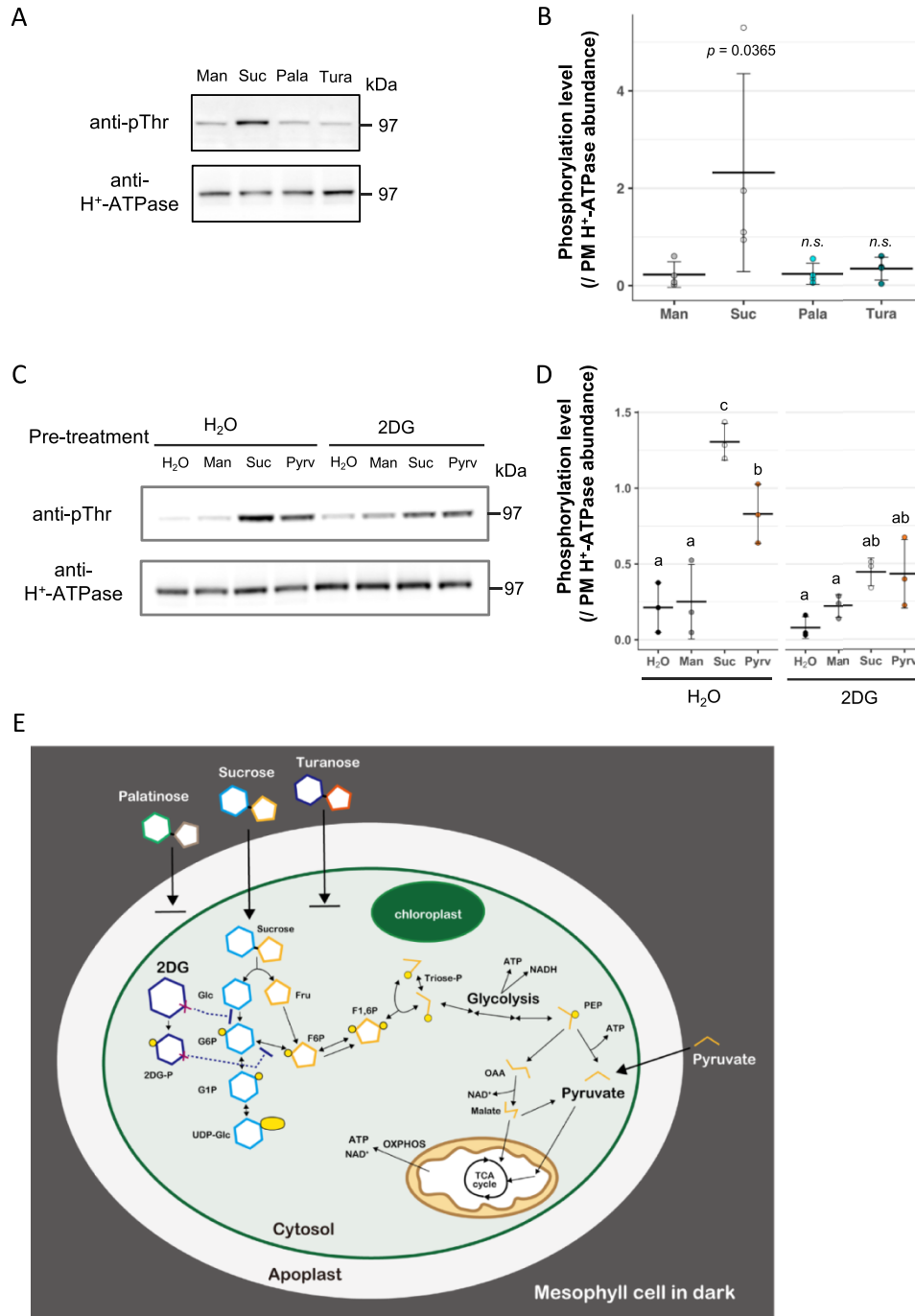
Fig. 1 PM H$^+$-ATPase phosphorylation induced by glycolysis and the downstream metabolites. (A) Phosphorylation of the penultimate Thr and abundance of PM H$^+$-ATPase in sucrose analog–supplemented pieces of leaves using anti-pThr and anti-PM H$^+$-ATPase antibodies, respectively. Suc, sucrose; Man, mannitol; Pala, palatinose; and Tura, turanose. (B) Phosphorylation of PM H$^+$-ATPase in sucrose analog–supplemented pieces of leaves. Crossbars and error bars represent the mean and SD of four independent experiments. *P*-values by one-way ANOVA with Dunnett's test compared to the control; n.s., not significant ($P > 0.05$). (C) Phosphorylation of penultimate Thr and abundance of PM H$^+$-ATPase in metabolite-supplemented pieces of leaves using anti-pThr and anti-PM H$^+$-ATPase antibodies. Pieces of leaves were preincubated with MilliQ H$_2$O or 2DG. Pyrv, pyruvate. (D) Phosphorylation of PM H$^+$-ATPase in metabolite-supplemented pieces of leaves. Crossbars and error bars represent the mean and SD of three independent experiments. Different letters above bars indicate significant differences by one-way ANOVA with the Tukey HSD test ($P < 0.05$). (E) Schematic of related metabolites and expected effects of sugar analogs. Exogenous sucrose metabolism in dark is shown. The unmetabolized sucrose analogs palatinose and turanose are not converted into hexoses intracellularly. 2DG is phosphorylated to 2DG-phosphate and competitively inhibits sucrose metabolism. Glc, glucose; Fru, fructose; G6P, glucose-6-phosphate; G1P, glucose-1-phosphate; F6P, fructose-6-phosphate; UDP-Glc, UDP-glucose; suc-6-P, sucrose-6-phosphate; F1,6P, fructose-1,6-bisphosphate; triose-P, triose-phosphate; PEP, phosphoenolpyruvate; OAA, oxaloacetate; OXPHOS, oxidative phosphorylation.
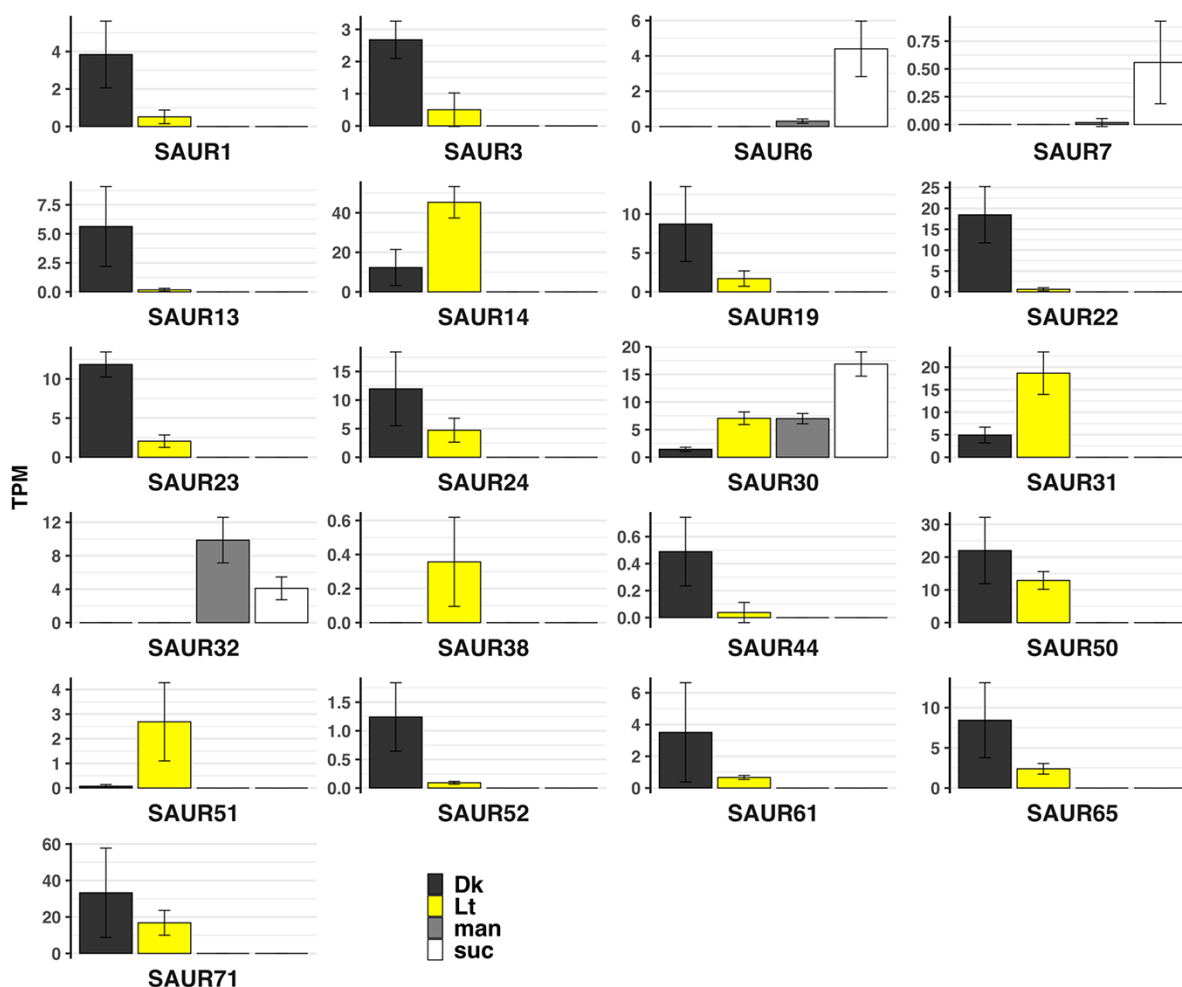
Fig. 2 Differentially expressed *SAUR* genes in leaves. TPM values of *SAUR* genes differentially expressed under the light or sucrose condition. Dk, dark for 30 min; Lt, light for 30 min; Man, 30 mM mannitol for 30 min and Suc, 30 mM sucrose for 30 min. Bars and error bars represent the mean and SD of four independent experiments.

positively affect the phosphorylation of PM H$^+$-ATPase in early response.

Interestingly, the SAUR30-GFP abundance was increased, and the band of SAUR30-GFP was shifted by the supplementation of sucrose to leaves and light illumination to seedlings and leaves (**Supplementary Figs. S6B, S7**), opening the possibility that the posttranslational regulation of SAUR30 protein may participate in early response.

Positive role of PM H$^+$-ATPase in light-dependent nitrate uptake

In illuminated leaves, N assimilation is triggered by the activation of nitrate reductase in response to photosynthesis (Kaiser and Huber 2001). In addition, PM H$^+$-ATPase generates an H$^+$ gradient across the PM, which supports several H$^+$ gradient-dependent transporters, including PM-localized NRTs (Hachiya and Sakakibara 2017). In line with the phosphorylation level of PM H$^+$-ATPase, the ATP hydrolysis activity of PM H$^+$-ATPase in illuminated leaves increases compared to dark conditions (Okumura et al. 2016). Therefore, we hypothesized

that light-induced PM H$^+$-ATPase activation in leaves acidifies apoplasts to generate an H$^+$ gradient and supports NRTs.

To test the above hypothesis, the nitrate uptake of leaves with different PM H$^+$-ATPase activities was investigated using 1 mM K^{15}NO$_3$ (**Fig. 6A**). As expected, illuminated leaves showed increased nitrate uptake compared to overnight dark-adapted leaves, whereas vanadate, an inhibitor of PM H$^+$-ATPase (Palmgren 2001), suppressed the increment of nitrate uptake under illumination (**Fig. 6B**). Moreover, the fungal toxin fusicoccin (Fc), an irreversible activator of PM H$^+$-ATPase, significantly increased nitrate uptake in dark (**Fig. 6C**). Although the relationship between PM H$^+$-ATPase activation and nitrate uptake needs to be further investigated at the molecular level, these results imply that the PM H$^+$-ATPase activation may have a positive role in light-dependent nitrate uptake in leaves.

Discussion

Photosynthesis- and photosynthetic-product–dependent phosphorylation of PM H$^+$-ATPase has been reported in
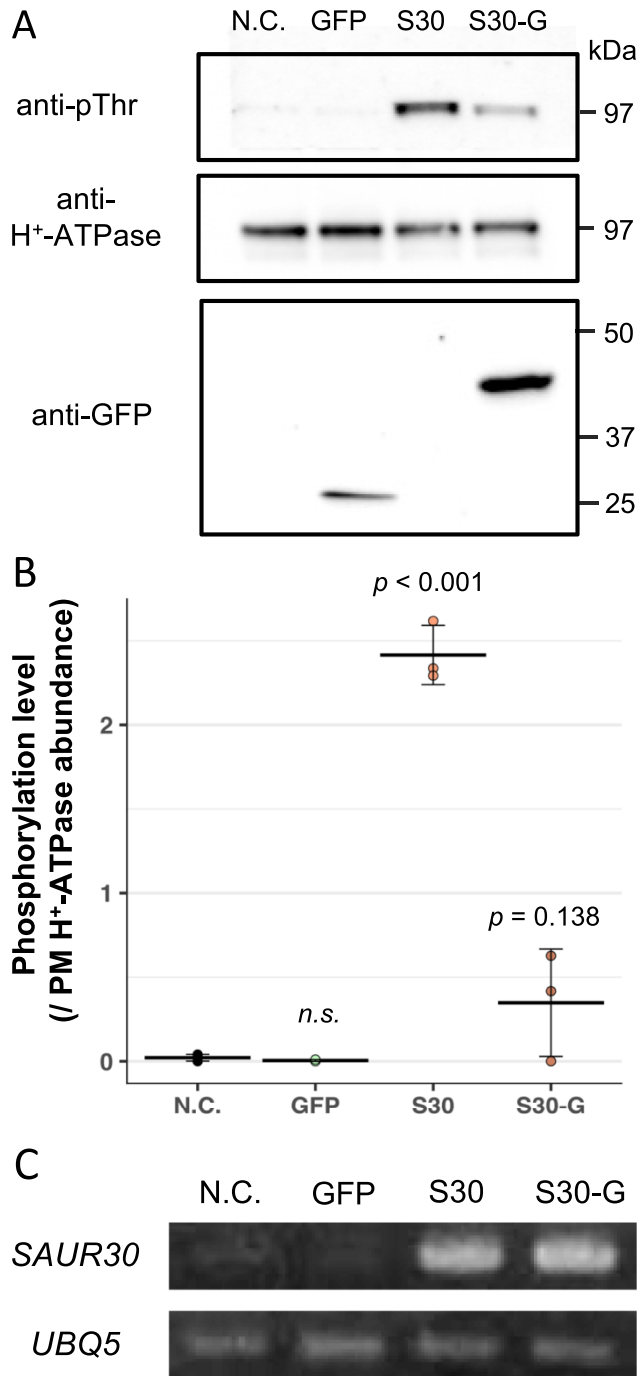
A

B

C

Fig. 3 SAUR30-induced PM H⁺-ATPase phosphorylation in MCPs. (A) Phosphorylation of the penultimate Thr and abundance of PM H⁺-ATPase in MCPs. The band at ∼25 kDa is GFP and that at 37–50 kDa is SAUR30-GFP. (B) Phosphorylation of PM H⁺-ATPase in transfected MCPs. Crossbars and error bars represent the mean and SD of three independent experiments. *P*-values by one-way ANOVA with Dunnet's test compared to the control; n.s., not significant ($P > 0.05$). (C) Detection of *SAUR30* overexpression in transfected MCPs by RT-PCR. *UBQ5* was used as the internal control.

thalli of *M. polymorpha* (Okumura et al. 2012a), protonemata of *P. patens* (Okumura et al. 2012b), the leaves of

A. thaliana and several vascular plant species (Okumura et al. 2016) and leaves of *Vallisneria gigantea* (Harada et al. 2020). Sucrose-dependent phosphorylation of PM H⁺-ATPase was also reported in *Arabidopsis* seedlings (Niittylä et al. 2007). Although photosynthesis- and photosynthetic-product–dependent phosphorylation of PM H⁺-ATPase is conserved among a wide range of plant species, the molecular mechanism and physiological role of the phosphorylation are unclear. Therefore, we used *Arabidopsis* leaves to evaluate the molecular mechanism and physiological role of photosynthesis-dependent PM H⁺-ATPase phosphorylation.

Our findings provide insight into the molecular mechanism and physiological role of PM H⁺-ATPase activation in leaves. First, photosynthetic products, especially of glycolysis and the downstream, are important for inducing PM H⁺-ATPase phosphorylation. Second, a novel isoform of SAUR genes, *SAUR30*, is implicated in the activation mechanism via SAUR-PP2C-D modules, but an as-yet-unknown early regulatory mechanism was also implied. Finally, we suggest that PM H⁺-ATPase activation via photosynthesis may have a positive role in light-dependent nitrate uptake in leaves (**Fig. 7**).

Glycolysis and the downstream metabolite may participate in photosynthesis-dependent PM H⁺-ATPase phosphorylation in leaves

Sucrose is predominantly produced in source leaves for translocation to other sink tissues and is responsible for disaccharide signaling in plant cells (Li and Sheen 2016). Palatinose and turanose are not metabolized in plants but induce the sucrose-specific signaling pathway (Fernie et al. 2001, Sinha et al. 2002). Palatinose is not recognized by the sucrose-proton symporter 2 (AtSUC2) transporter, a possible sucrose signal receptor, whereas turanose is recognized by the AtSUC2 transporter (Chandran et al. 2003). Only sucrose induced phosphorylation of PM H⁺-ATPase (**Fig. 1A**, **B**). Therefore, the sucrose-specific signaling pathway is not involved in PM H⁺-ATPase phosphorylation.

Next, the involvement of hexose and hexose phosphate signaling was investigated. Intracellular hexose availability is perceived by hexokinase (Li and Sheen 2016). To mimic the intracellular accumulation of hexose and hexose phosphate, the glucose analog 2DG was applied to leaves. 2DG is phosphorylated intracellularly and perceived by hexokinase (Klein and Stitt 1998, Li and Sheen 2016). Supplementation of 2DG alone had no effect (**Fig. 1C**, **D**), indicating that PM H⁺-ATPase phosphorylation is independent of hexose accumulation and the hexose phosphate pool.

In addition, 2DG inhibits glycolysis in cancer cells (Pajak et al. 2020) and plant seedlings (Xiong et al. 2013). 2DG-pretreated leaves showed decreased PM H⁺-ATPase phosphorylation with exogenous supplementation of sucrose, and pyruvate alone induced PM H⁺-ATPase phosphorylation (**Fig. 1C**, **D**). Therefore, respiration C metabolites may be responsible for phosphorylation of PM H⁺-ATPase, but not sugar production. This is consistent with the transcriptome analysis results, implying
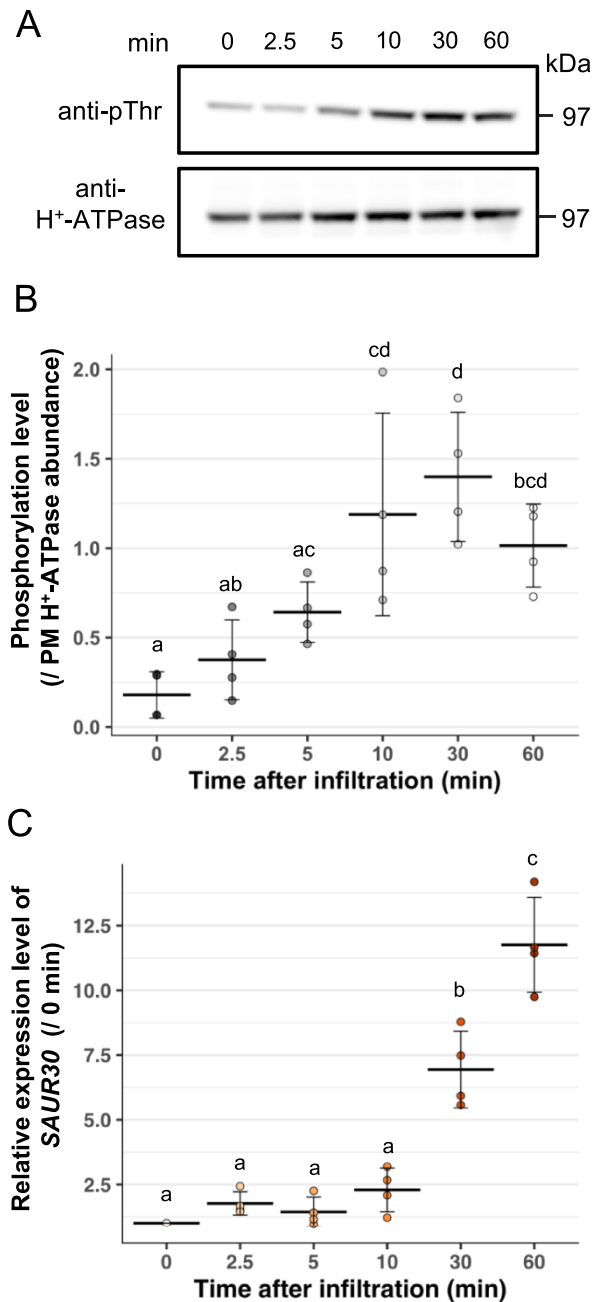
Fig. 4 Temporal difference between phosphorylation of PM H$^+$-ATPase and expression of *SAUR30* in sucrose-supplemented leaves. (A) Phosphorylation of the penultimate Thr and abundance of PM H$^+$-ATPase in pieces of leaves supplemented with sucrose as determined using anti-pThr and anti-PM H$^+$-ATPase antibodies. (B) Phosphorylation of PM H$^+$-ATPase in pieces of leaves supplemented with sucrose. Pieces of leaves were flash-frozen at the indicated times after infiltration. Crossbars and error bars represent the mean and SD of four independent experiments. Different letters above bars indicate significant differences by one-way ANOVA with the Tukey HSD test ($P < 0.05$). (C) Expression of *SAUR30* in pieces of leaves supplemented with sucrose. Pieces of leaves were flash-frozen at the indicated times after infiltration. *UBQ5* was used as the internal control. Crossbars and error bars represent the mean and SD of four independent experiments. Different letters above bars indicate significant differences by one-way ANOVA with the Tukey HSD test ($P < 0.05$).

that dark-adapted plants recovered from energy starvation after light illumination or sucrose supplementation (**Supplementary Fig. S2**). However, this is tentative because the C flux in illuminated leaves differs from that of leaves in dark.

In illuminated leaves, mitochondrial pyruvate dehydrogenase (PDH; AT1G53240), a rate-limiting enzyme of pyruvate conversion into acetyl-coenzyme A in mitochondria and the entry point to the tricarboxylic acid (TCA) cycle, is inhibited by transcriptional modification and PTM (Zhang et al. 2021b). Therefore, the TCA cycle is limited due to the inactivation of PDH in illuminated leaves (Sweetlove et al. 2010). Isotope-labeled C flux analysis revealed that several photosynthesis, glycolysis and noncyclic TCA reaction metabolites are produced within 20 min of illumination—2-phosphoglyceric acid, pyruvate, alanine, serine and trehalose (Szecowka et al. 2013). Together with the previous report that PM H$^+$-ATPase phosphorylation is induced after 15–30 min of illumination (Okumura et al. 2016), the finding that 2DG pretreatment suppressed sucrose-dependent phosphorylation of PM H$^+$-ATPase in dark (**Fig. 1C, D**) implicates glycolysis and the downstream metabolites in illuminated leaves in photosynthesis-dependent phosphorylation of PM H$^+$-ATPase. Studies using inducible mutants that can transiently alter the specific related metabolic pathway may provide further insight.

Additionally, the effect of 2DG may not be limited to glycolysis inhibition because the pyruvate-induced phosphorylation of PM H$^+$-ATPase was partially, but not significantly, affected (**Fig. 1C, D**). In mammalian cells, the treatment of 2DG may not affect only glycolysis but also the metabolism in mitochondria (Pietzke et al. 2014). Therefore, a quantitative metabolome analysis using 2DG-treated leaves and revealing the effect of 2DG in plant cells may give further insights into the key metabolites of glycolysis and downstream in phosphorylation of PM H$^+$-ATPase.

Two temporal mechanisms of PM H$^+$-ATPase in *Arabidopsis* leaves

Several SAUR proteins activate PM H$^+$-ATPase by inhibiting the PP2C-D (Ren et al. 2018). Although many *SAUR* genes are responsive to auxin, *SAUR30* is not responsive (Paponov et al. 2008). Online transcriptome database shows that *SAUR30* is expressed in most of tissues and responsive to abscisic acid in MCPs (**Supplementary Fig. S4**). However, we found that *SAUR30* is likely responsive to photosynthetic products and is the most abundant *SAUR* in sucrose-supplemented leaves (**Fig. 2**). Furthermore, transient expression of *SAUR30* in MCPs induced phosphorylation of endogenous PM H$^+$-ATPase via inhibiting PP2C-Ds (**Fig. 3, Supplementary Fig. S5**), as well as that SAUR30-GFP OE seedlings and plants showed a higher level of PM H$^+$-ATPase phosphorylation (**Fig. 5, Supplementary Fig. S6B**), suggesting that photosynthesis-dependent expression of *SAUR30* maintains the high phosphorylation level of PM H$^+$-ATPase in leaves. Other *SAUR* family genes, which were excluded from our analysis due to high FDR values, may function redundantly with *SAUR30*. Other DEGs found in both light and sucrose conditions may also participate in the pathway.
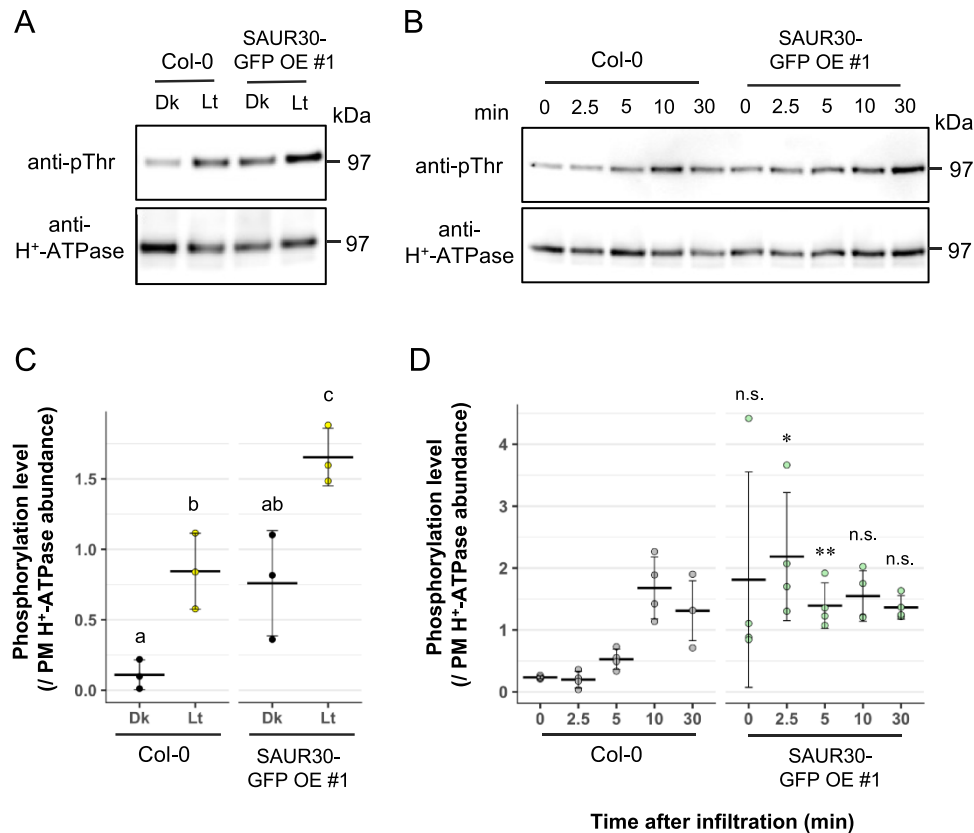
Fig. 5 Earlier induction of PM H⁺-ATPase phosphorylation in SAUR30-GFP overexpression plants. (A) Phosphorylation of the penultimate Thr and abundance of PM H⁺-ATPase in illuminated pieces of leaves of Col-0 or SAUR30-GFP overexpression plants using anti-pThr and anti-PM H⁺-ATPase antibodies, respectively. Plants were illuminated for 30 min, and the pieces of leaves were harvested. (B) Time-course change of phosphorylation of the penultimate Thr and abundance of PM H⁺-ATPase in sucrose-supplemented pieces of leaves of Col-0 or SAUR30-GFP overexpression plants using anti-pThr and anti-PM H⁺-ATPase antibodies, respectively. Infiltration with 30 mM sucrose. Pieces of leaves were flash-frozen at the indicated times after infiltration. (C) Phosphorylation of PM H⁺-ATPase in illuminated pieces of leaves of Col-0 or SAUR30-GFP overexpression plants. Crossbars and error bars represent the mean and SD of three independent experiments. Different letters above bars indicate significant differences by one-way ANOVA with the Tukey HSD test ($P < 0.05$). (D) Time-course change of phosphorylation of PM H⁺-ATPase in sucrose-supplemented pieces of leaves of Col-0 or SAUR30-GFP overexpression plants. Crossbars and error bars represent the mean and SD of four independent experiments. Asterisk indicates the significant difference in the phosphorylation level between two genotypes at the same time point. *P*-values by Welch's two-sample *t*-test; n.s., not significant ($P > 0.05$); *$P < 0.05$ and **$P < 0.025$.

Notably, induction of *SAUR30* expression in sucrose-supplemented leaves occurred later than PM H⁺-ATPase phosphorylation (**Fig. 4**), implying the involvement of an unknown early responsive mechanism (5–10 min) of PM H⁺-ATPase phosphorylation in leaves. Interestingly, the SAUR30-GFP OE plant showed that the abundance of SAUR30-GFP was increased, and the band was shifted by light illumination and supplementation of sucrose in leaves (**Supplementary Fig. S7**). Both abundance change and band shift were observed 2.5 min after the infiltration of sucrose at the same time point as PM H⁺-ATPase phosphorylation (**Fig. 5B**, **Supplementary Fig. S7B, D**), implying that the SAUR30 protein may participate in the early response of PM H⁺-ATPase to photosynthetic products. Therefore, it is possible that PTM-dependent stabilization and activation of SAUR30 proteins by photosynthetic products induce phosphorylation of PM H⁺-ATPase as soon as photosynthesis occurs, which is subsequently (>10 min) supported by the increment of *SAUR30* transcript level. Although light-induced stabilization of SAUR63 protein is reported (Chae et al. 2012), to our knowledge, this is the first time to report the band shift of SAUR protein in response to light illumination and photosynthetic products. Further investigation of PTM-dependent regulation of SAUR protein in leaves with sucrose supplementation may provide mechanistic insights.

Possible role of PM H⁺-ATPase in light-dependent nitrate uptake of leaves

To dissect the physiological importance of PM H⁺-ATPase activation in leaves, we investigated the relationship between photosynthesis-dependent PM H⁺-ATPase activation and N assimilation in illuminated leaves, because photosynthesis and N assimilation are closely associated. Synthesis of major components of the photosynthesis machinery—including chlorophyll,
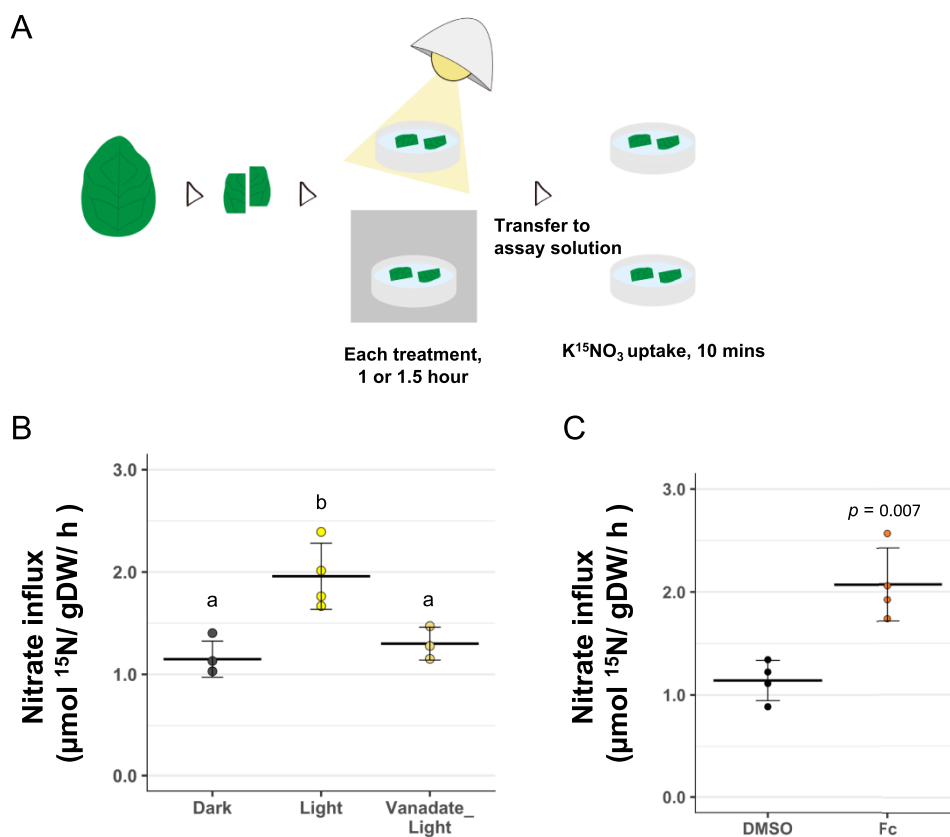
Fig. 6 Light- and PM H$^+$-ATPase–dependent nitrate uptake in leaves. (A) Schematic of nitrate uptake assay. Leaves of overnight dark-adapted plants were harvested and cut in half, removing the main vein, and floated on H$_2$O for dark and light samples. Pieces of leaves for 1 mM vanadate ammonium were floated in 0.5 mM MES–KOH (pH 5.6). For light and Vanadate_Light treatment, pieces of leaves were incubated for 30 min in dark and illuminated for 1 h. Pieces of leaves for DMSO control and 10 μM Fc in DMSO (Sigma-Aldrich) were floated in 0.5 mM MES–KOH (pH 5.6) and incubated for 1.5 h in dark. After treatment, pieces of leaves were transferred to 1 mM K^{15}NO$_3$ assay solution and incubated for 10 min. (B) Nitrate influx in leaves treated with dark, light and a PM H$^+$-ATPase inhibitor followed by light (Vanadate_Light). Crossbars and error bars represent the mean and SD of three to four independent experiments. Different letters above bars indicate significant differences by one-way ANOVA with the Tukey test ($P < 0.05$). (C) Nitrate influx in leaves treated with DMSO control or a PM H$^+$-ATPase activator, Fc in dark. Crossbars and error bars represent the mean and SD of four independent experiments. P-values by Welch's two-sample t-test.

light-harvesting complex, Rubisco and ATP synthase—in chloroplasts requires large amounts of N (Evans and Clarke 2019). In addition, the photosynthesis rate is significantly affected by N availability (Perchlik and Tegeder 2018). PM H$^+$-ATPase generates an H$^+$ gradient across the PM. The activity of H$^+$-coupled nutrient transporters is dependent on the PM potential and H$^+$ gradient (Palmgren 2001, Sondergaard et al. 2004). Therefore, we hypothesized that PM H$^+$-ATPase activated by photosynthesis energizes PM-localized NRTs, such as NRT proteins. Although our stable isotope–labeled nitrate (^{15}NO$_3^-$) uptake assay with pieces of leaves did not demonstrate direct evidence of involvement of NRT proteins nor actual cellular nitrate influx across PM, the nitrate uptake assay using cut pieces of leaves implies that light-induced increment of nitrate uptake was dependent on PM H$^+$-ATPase activity (**Fig. 6**).

It has been suggested that transportation of N requires the PM H$^+$-gradient and membrane potential in leaves of some plants including *Arabidopsis* and N-starved cucumber (Cookson et al. 2005, Nikolic et al. 2012); however, there is no direct evidence that PM H$^+$-ATPase activation is involved in light-dependent nitrate uptake in leaves under nutrient sufficient condition. From our results, we speculate that energy production from photosynthesis activates PM H$^+$-ATPase and thus nitrate uptake to maintain high N availability in leaves (**Fig. 7**). The finding illustrates that photosynthesis-dependent nitrate uptake in illuminated leaves is an interesting case of the C–N interaction. Since the molecular mechanism and physiological role of PM H$^+$-ATPase activation in the context of C N interactions have never been demonstrated, our finding may provide a novel insight into the molecular mechanism of the C–N interaction in plant leaves.
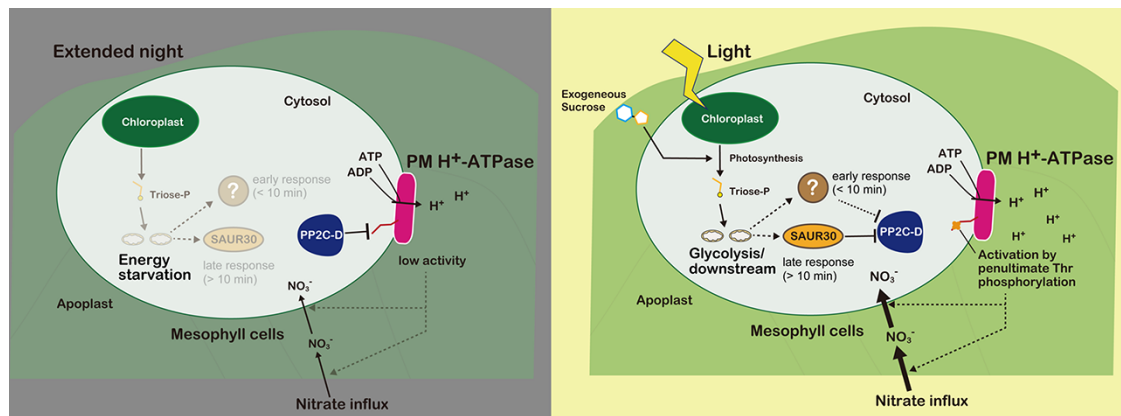
Fig. 7 Hypothetical model of the mechanism and physiological role of PM H$^+$-ATPase activation in leaves. Photosynthesis generates triose-phosphate in illuminated leaves and glycolysis, and the downstream metabolites induce the unknown activating mechanism within 5–10 min (early response) and the SAUR30 expression after 10 min (late response). The inductions inhibit PP2C-D, leading to the high phosphorylation level of PM H$^+$-ATPase. Activated PM H$^+$-ATPase creates an H$^+$ gradient across the PM. The H$^+$ gradient may facilitate nitrate uptake into leaves. In early response, PTM of SAUR30 protein may support the activating mechanism.

Materials and Methods

Plant materials and growth conditions

Arabidopsis thaliana accession Columbia-0 (Col-0) was used as the wild-type plant. Seeds were imbibed with tap H$_2$O and stratified at 4°C for 3–4 d. Plants were grown in soil at 23°C under a 16-h light:8-h dark cycle (6:00 h to 22:00 h light) with a photon flux of 50–100 μmol m^{-2} s^{-1}. Soil was kept moistened and nutrition-rich by regular watering and fertilizer applications. Four- to five-week-old plants were transferred to a dark room for dark adaptation between 17:00 h and 18:00 h (ZT11 to ZT12), and leaves were harvested or treated between 11:00 h and 13:00 h (18–20 h after the start of dark adaptation).

Exogenous supplementation of C metabolites to leaves

Fully expanded leaves (30–60 mg fresh weight) were harvested from overnight dark-adapted plants and cut into two pieces, removing the main veins, upper edges and lower edges. For sucrose analog supplementation, four pieces of leaves for each treatment were floated on MilliQ H$_2$O containing 30 mM mannitol (Nacalai), 30 mM sucrose (Nacalai), 30 mM turanose (Sigma) or 30 mM palatinose (Sigma) for 30 min.

For 2DG supplementation, four pieces of leaves were floated on H$_2$O containing (or not) 30 mM 2-deoxy-D-glucose (Nacalai) for 1 h. Pieces of leaves were infiltrated in a syringe with H$_2$O containing (or not) 60 mM mannitol, 30 mM sucrose or 30 mM pyruvate-sodium (animal-free; Nacalai) and were floated on each solution for 30 min.

For the sucrose time-course experiment, four pieces of leaves were infiltrated in a syringe with H$_2$O containing 30 mM sucrose. Pieces of leaves were floated on the same sucrose solution and collected at the indicated times.

Immunoblotting

Pieces of leaves were collected in tubes and flash-frozen in liquid N. Frozen leaf samples were homogenized using a pestle in solubilization buffer [2% (w/v) sodium dodecyl sulfate (SDS), 1 mM EDTA, 20% (v/v) glycerol, 10 mM Tris (hydroxymethyl) aminomethane-HCl (pH 6.8), 0.012% (w/v) CBB, 50 mM dithiothreitol, 1 mM phenylmethylsulfonyl fluoride, 2.5 mM NaF, 20 μM leupeptin (Leu)]. Solubilized samples were centrifuged at 14,000×*g* and 25°C for 5 min.

For the MCP sample, solubilization buffer was added to frozen MCPs. Identical volumes of supernatants were subjected to 9% SDS–polyacrylamide gel electrophoresis.

Immunoblotting was performed as described previously (Hayashi et al. 2010). Anti-H$^+$-ATPase, anti-pThr and anti-GFP (Roche; monoclonal) antibodies were used to evaluate the abundance of PM H$^+$-ATPase, phosphorylated penultimate Thr of PM H$^+$-ATPase (pThr) and GFP-fused SAUR30, respectively. The specificity of each antibody is shown in **Supplementary Fig. S3**.

Phosphorylation of PM H$^+$-ATPase was determined based on band densities on anti-pThr and anti-PM H$^+$-ATPase immunoblots using ImageJ software (version 1.53 f51).

RNA extraction and complementary DNA synthesis

For RNA-seq, overnight dark-adapted *Arabidopsis* leaves were subjected to white-light illumination (Lt) or incubation with 30 mM sucrose solution (Suc) or mannitol (Man) for 30 min. Reference control samples for the Lt and Suc conditions were dark-adapted (Dk) and Man conditions, respectively. Total RNAs were extracted from leaves using NucleoSpin RNA Plant (Macherey-Nagel) according to the manufacturer's instructions. For RT-quantitative PCR, 400 ng of purified RNA was subjected to reverse transcription using the PrimeScriptRT Reagent Kit (TaKaRa).

The extraction of RNA and synthesis of complementary DNA (cDNA) from MCPs (approximately 400 MCPs) were performed using a SuperScript IV CellsDirect cDNA Synthesis Kit (Invitrogen) according to the manufacturer's instructions.

Preparation of complementary DNA libraries and RNA-seq

A TruSeq RNA Sample Prep Kit v. 2 (Illumina) was used for the construction of complementary DNA libraries, and the complementary DNA libraries were sequenced on a NextSeq 500 system (Illumina). NextSeq 500 pipeline software was used for base calling of sequence reads. The reads used for mapping were selected by the length of 50 continuous nucleotides with quality values of >25. The selected reads were mapped to *A. thaliana* transcripts using Bowtie software. Experiments in all conditions were repeated four times, independently; 11.3–22.2 million total reads per experiment were obtained. Gene-expression values are reported as TPM and log$_2$ (fold change) values. Normalization of read counts and statistical analyses was performed using EdgeR software in

the Degust v. 3.1.0 web tool, R software (v. 4.0.3) and R studio (v. 1.4.110). Values of FDR < 0.05 and $\log_2(|\text{fold change}|) > 1$ were used as cutoffs for selecting DEGs. Reference transcriptome data were from KIN10-dependent genes (Baena-González et al. 2007).

Preparation and transfection of MCPs

For the construction of transient expression plasmids, the coding sequence of *SAUR30* was cloned using Prime STAR MAX polymerase mix (TaKaRa) and the gene-specific primers as shown in **Supplementary Table S1**. Amplified fragments were inserted into the pUC18 vector containing pro35S:sGFP:NOS terminator by infusion (TaKaRa). Before transfection, plasmids were purified from overnight-cultured competent *Escherichia coli* (DH5α) using a PureYield Plasmid Midiprep System (Promega) and the phenol–chloroform method.

Enzymatic preparation of MCPs and PEG–Ca^{2+} transfection was conducted as described previously (Yoo et al. 2007) with minor modification. Briefly, mature leaves were harvested from 4- to 5-week-old plants, and cell walls were enzymatically digested in a solution of Cellulase R-10 (Yakult) and Macerozyme R-10 (Yakult) for 2.5 h. Isolated MCPs (5.0×10^4 protoplasts) in MMg [0.4 M mannitol, 4 mM 2-(*N*-morpholilino)ethanesulfonic acid (MES)–KOH (pH 5.7), 15 mM $MgCl_2$] were transfected with the purified plasmids (20–30 μg) by adding an equal volume of PEG–calcium solution [40% PEG4000 (Sigma-Aldrich), 0.2 M mannitol, 100 mM $CaCl_2$] for 5–6 min. After transfection, MCPs were washed three times and incubated in MKCa solution [0.4 M mannitol, 2 mM MES–KOH (pH 5.7), 20 mM KCl, 1 mM $CaCl_2$] in 12-well plates for 4.5 h. Finally, MCPs were collected and stored at −80°C until immunoblotting.

RT-PCR and quantitative PCR

Detection of *SAUR30* and *UBQ5* expression in MCPs was performed using ExTaq polymerase (TaKaRa), and quantification of *SAUR30* and *UBQ5* expression in sucrose-supplemented leaves was performed using SYBR Green PCR Master Mix (Applied Biosystems), a StepOnePlus™ RT-PCR System (Applied Biosystems), and the gene-specific primers are listed in **Supplementary Table S1**.

Generation of transgenic overexpression plants

For the construction of plasmid for the plant transformation, the sequence of SAUR30-GFP was cloned from the transient expression plasmid with the primer in **Supplementary Table S1** and inserted to the pENTR entry vector using NotI and AscI by infusion. The constructed entry vector was replaced with the pGWB405 binary vector (Nakagawa et al. 2007) using LR Clonase II (Invitrogen).

Wild-type plants were transformed with *Agrobacterium tumefaciens* strain GV3101 by the floral dip method (Clough and Bent 1998). Transformants were selected by antibiotics and expression levels, and the two most highly expressed lines (OEs #1 and #2) were used in the study.

Stable isotope–labeled nitrate uptake assay

Six pieces of leaves for each treatment from overnight dark-adapted plants were washed with H_2O and floated on MilliQ H_2O for no-$K^{15}NO_3$ control, dark and light samples. Pieces of leaves for 1 mM vanadate ammonium were floated in MES–KOH (pH 5.6). For light and Vanadate_Light treatment, pieces of leaves were incubated for 30 min in dark and illuminated (50–100 μmol m^{-2} s^{-1}) for 1 h. Pieces of leaves for dimethyl sulfoxide (DMSO) control and 10 μM Fc in DMSO (Sigma-Aldrich) were floated in MES–KOH (pH 5.6) and incubated for 1.5 h in dark.

Treated leaves were transferred to assay solution, 1 mM $K^{15}NO_3$ (atom% ^{15}N: 99%) in H_2O, and incubated for 10 min, except for the no-$K^{15}NO_3$ control. Incubated leaves were washed twice in a large volume of H_2O and collected into tubes. The samples were dried at 70°C for at least 20 h, and the total N [%g dry weight (DW)] and ^{15}N (atom%) contents were analyzed using a

Flash2000-DELTAplus Advantage ConFloIII System (ThermoFisher Scientific) at Shoko Science Co., Ltd, Yokohama, Japan.

Influx of $^{15}NO_3$ (μmol/gDW/h) was calculated, using the total N (%gDW) and ^{15}N content (atom%) of sample. ^{15}N contents (atom%) of sample were obtained, subtracting the ^{15}N contents (atom%) of no-^{15}NO treated control from the measured ^{15}N contents value of sample.

Data analysis and statistics

Plots were generated and statistical analyses were conducted using R studio with the ggplot2 and multcomp packages, respectively. Welch's *t*-test was conducted for two-sample comparison. Analysis of variance (ANOVA) was conducted before a Tukey honestly significant difference (HSD) or Dunnett's post hoc test. The statistical results are listed in **Supplementary Data File S2**.

Supplementary Data

Supplementary data are available at *PCP* online.

Data Availability

All data that support the findings of this study are included in the manuscript and Supplementary data of this article. The raw data in this study are available from the corresponding author upon the request. RNA-seq raw data have been deposited in the DNA Data Bank of Japan Sequenced Read Archive under the accession number DRA012961: SAUR1, AT4G34770; SAUR3, AT4G34790; SAUR6, AT2G21210; SAUR7, AT2G21200; SAUR13, AT4G38825; SAUR14, AT4G38840; SAUR19, AT5G18010; SAUR22, AT5G18050; SAUR23, AT5G18060; SAUR24, AT5G 18080; SAUR30, AT5G53590; SAUR31, AT4G00880; SAUR32, AT2G46690; SAUR38, AT2G24400; SAUR44, AT5G03310; SAU R50, AT4G34760; SAUR51, AT1G75580; SAUR52, AT1G75590; SAUR61, AT1G29420; SAUR63, AT1G29440; SAUR65, AT1G 29460; and SAUR71, AT1G56150

Author Contributions

S.N.K. and T.K. designed the research; S.N.K. and T.S. performed the research and analyzed data. All authors contributed to the writing of the paper and reviewed the paper.

Disclosures

The authors have no conflicts of interest to declare.

References

Akiyama, M., Sugimoto, H., Inoue, S., Takahashi, Y., Hayashi, M., Hayashi, Y., et al. (2022) Type 2C protein phosphatase clade D family members dephosphorylate guard cell plasma membrane H$^+$-ATPase. *Plant Physiol.* 188: 2228–2240.

Assmann, S.M., Simoncini, L. and Schroeder, J.I. (1985) Blue light activates electrogenic ion pumping in guard cell protoplasts of *Vicia faba*. *Nature* 318: 285–287.

Baena-González, E., Rolland, F., Thevelein, J.M. and Sheen, J. (2007) A central integrator of transcription networks in plant stress and energy signalling. *Nature* 448: 938–942.

Chae, K., Isaacs, C.G., Reeves, P.H., Maloney, G.S., Muday, G.K., Nagpal, P., et al. (2012) *Arabidopsis* SMALL AUXIN UP RNA63 promotes hypocotyl and stamen filament elongation. *Plant J.* 71: 684–697.

Chandran, D., Reinders, A. and Ward, J.M. (2003) Substrate specificity of the *Arabidopsis thaliana* sucrose transporter AtSUC2. *J. Biol. Chem.* 278: 44320–44325.

Clough, S.J. and Bent, A.F. (1998) Floral dip: a simplified method for Agrobacterium-mediated transformation of *Arabidopsis thaliana*. *Plant J.* 16: 735–743.

Cookson, S.J., Williams, L.E. and Miller, A.J. (2005) Light-dark changes in cytosolic nitrate pools depend on nitrate reductase activity in *Arabidopsis* leaf cells. *Plant Physiol.* 138: 1097–1105.

de Bont, L., Naim, E., Arbelet-Bonnin, D., Xia, Q., Palm, E., Meimoun, P., et al. (2019) Activation of plasma membrane H$^+$-ATPases participates in dormancy alleviation in sunflower seeds. *Plant Sci.* 280: 408–415.

Delhon, P., Gojon, A., Tillard, P. and Passama, L. (1996) Diurnal regulation of NO$_3^-$ uptake in soybean plants IV. Dependence on current photosynthesis and sugar availability to the roots. *J. Exp. Bot.* 47: 893–900.

DeWitt, N.D. and Sussman, M.R. (1995) Immunocytological localization of an epitope-tagged plasma membrane proton pump (H$^+$-ATPase) in phloem companion cells. *Plant Cell* 7: 2053–2067.

Evans, J.R. and Clarke, V.C. (2019) The nitrogen cost of photosynthesis. *J. Exp. Bot.* 70: 7–15.

Falhof, J., Pedersen, J.T., Fuglsang, A.T. and Palmgren, M. (2016) Plasma membrane H$^+$-ATPase regulation in the center of plant physiology. *Mol. Plant* 9: 323–337.

Fernie, A.R., Roessner, U. and Geigenberger, P. (2001) The sucrose analog palatinose leads to a stimulation of sucrose degradation and starch synthesis when supplied to discs of growing potato tubers. *Plant Physiol.* 125: 1967–1977.

Hachiya, T. and Sakakibara, H. (2017) Interactions between nitrate and ammonium in their uptake, allocation, assimilation, and signaling in plants. *J. Exp. Bot.* 68: 2501–2512.

Harada, A., Okazaki, Y., Kinoshita, T., Nagai, R. and Takagi, S. (2020) Role of proton motive force in photoinduction of cytoplasmic streaming in *Vallisneria* mesophyll cells. *Plants* 9: 376.

Haruta, M., Burch, H.L., Nelson, R.B., Barrett-Wilt, G., Kline, K.G., Mohsin, S.B., et al. (2010) Molecular characterization of mutant *Arabidopsis* plants with reduced plasma membrane proton pump activity. *J. Biol. Chem.* 285: 17918–17929.

Hayashi, Y., Nakamura, S., Takemiya, A., Takahashi, Y., Shimazaki, K. and Kinoshita, T. (2010) Biochemical characterization of in vitro phosphorylation and dephosphorylation of the plasma membrane H$^+$-ATPase. *Plant Cell Physiol.* 51: 1186–1196.

Hoffmann, R.D., Portes, M.T., Olsen, L.I., Damineli, D.S.C., Hayashi, M., Nunes, C.O., et al. (2020) Plasma membrane H$^+$-ATPases sustain pollen tube growth and fertilization. *Nature Commun.* 11: 2395.

Inoue, S. and Kinoshita, T. (2017) Blue light regulation of stomatal opening and the plasma membrane H$^+$-ATPase. *Plant Physiol.* 174: 531–538.

Kaiser, W.M. and Huber, S.C. (2001) Post-translational regulation of nitrate reductase: mechanism, physiological relevance and environmental triggers. *J. Exp. Bot.* 52: 1981–1989.

Kinoshita, T. and Shimazaki, K. (1999) Blue light activates the plasma membrane H$^+$-ATPase by phosphorylation of the C-terminus in stomatal guard cells. *EMBO J.* 18: 5548–5558.

Klein, D. and Stitt, M. (1998) Effects of 2-deoxyglucose on the expression of rbcS and the metabolism of *Chenopodium rubrum* cell-suspension cultures. *Planta* 205: 223–234.

Li, L. and Sheen, J. (2016) Dynamic and diverse sugar signaling. *Curr. Opin. Plant Biol.* 33: 116–125.

Lupini, A., Araniti, F., Mauceri, A., Princi, M.P., Sorgonà, A., Sunseri, F., et al. (2018) Coumarin enhances nitrate uptake in maize roots through modulation of plasma membrane H$^+$-ATPase activity. *Plant Biol.* 20: 390–398.

Matt, P., Geiger, M., Walch-Liu, P., Engels, C., Krapp, A. and Stitt, M. (2001) The immediate cause of the diurnal changes of nitrogen metabolism in leaves of nitrate-replete tobacco: a major imbalance between the rate of nitrate reduction and the rates of nitrate uptake and ammonium metabolism during the first part of the light period. *Plant Cell Environ.* 24: 177–190.

Minami, A., Takahashi, K., Inoue, S., Tada, Y. and Kinoshita, T. (2019) Brassinosteroid induces phosphorylation of the plasma membrane H$^+$-ATPase during hypocotyl elongation in *Arabidopsis thaliana*. *Plant Cell Physiol.* 60: 935–944.

Nakagawa, T., Suzuki, T., Murata, S., Nakamura, S., Hino, T., Maeo, K., et al. (2007) Improved gateway binary vectors: high-performance vectors for creation of fusion constructs in transgenic analysis of plants. *Biosci. Biotechnol. Biochem.* 71: 2095–2100.

Niittylä, T., Fuglsang, A.T., Palmgren, M.G., Frommer, W.B. and Schulze, W.X. (2007) Temporal analysis of sucrose-induced phosphorylation changes in plasma membrane proteins of *Arabidopsis*. *Mol. Cell Proteom.* 6: 1711–1726.

Nikolic, M., Cesco, S., Monte, R., Tomasi, N., Gottardi, S., Zamboni, A., et al. (2012) Nitrate transport in cucumber leaves is an inducible process involving an increase in plasma membrane H$^+$-ATPase activity and abundance. *BMC Plant Biol.* 12: 2–13.

Okumura, M., Inoue, S., Kuwata, K. and Kinoshita, T. (2016) Photosynthesis activates plasma membrane H$^+$-ATPase via sugar accumulation. *Plant Physiol.* 171: 580–589.

Okumura, M., Inoue, S., Takahashi, K., Ishizaki, K., Kohchi, T. and Kinoshita, T. (2012a) Characterization of the plasma membrane H$^+$-ATPase in the liverwort *Marchantia polymorpha*. *Plant Physiol.* 159: 826–834.

Okumura, M., Takahashi, K., Inoue, S. and Kinoshita, T. (2012b) Evolutionary appearance of the plasma membrane H$^+$-ATPase containing a penultimate threonine in the bryophyte. *Plant Sig. Behav.* 7: 7–11.

Pajak, B., Siwiak, E., Sołtyka, M., Priebe, A., Zieliński, R., Fokt, I., et al. (2020) 2-Deoxy-D-glucose and its analogs: from diagnostic to therapeutic agents. *Int. J. Mol. Sci.* 21: 234.

Palmgren, M.G. (2001) Plant plasma membrane H$^+$-ATPases: powerhouses for nutrient uptake. *Annu. Rev. Plant Physiol. Plant Mol. Biol.* 52: 817–845.

Paponov, I.A., Paponov, M., Teale, W., Menges, M., Chakrabortee, S., Murray, J.A.H., et al. (2008) Comprehensive transcriptome analysis of auxin responses in *Arabidopsis*. *Mol. Plant* 1: 321–337.

Perchlik, M. and Tegeder, M. (2018) Leaf amino acid supply affects photosynthetic and plant nitrogen use efficiency under nitrogen stress. *Plant Physiol.* 178: 174–188.

PCP
PLANT & CELL PHYSIOLOGY

Pietzke, M., Zasada, C., Mudrich, S. and Kempa, S. (2014) Decoding the dynamics of cellular metabolism and the action of 3-bromopyruvate and 2-deoxyglucose using pulsed stable isotope-resolved metabolomics. *Cancer Metab.* 2: 9.

Ren, H., Park, M.Y., Spartz, A.K., Wong, J.H. and Gray, W.M. (2018) A subset of plasma membrane-localized PP2C.D phosphatases negatively regulate SAUR-mediated cell expansion in *Arabidopsis*. *PLoS Genet.* 14: e1007455.

Robertson, W.R., Clark, K., Young, J.C. and Sussman, M.R. (2004) An *Arabidopsis thaliana* plasma membrane proton pump is essential for pollen development. *Genetics* 168: 1677–1687.

Sinha, A.K., Hofmann, M.G., Römer, U., Köckenberger, W., Elling, L. and Roitsch, T. (2002) Metabolizable and non-metabolizable sugars activate different signal transduction pathways in tomato. *Plant Physiol.* 128: 1480–1489.

Sondergaard, T.E., Schulz, A. and Palmgren, M.G. (2004) Energization of transport processes in plants. Roles of the plasma membrane H^+-ATPase. *Plant Physiol.* 136: 2475–2482.

Spartz, A.K., Lee, S.H., Wenger, J.P., Gonzalez, N., Itoh, H., Inzé, D., et al. (2012) The SAUR19 subfamily of SMALL AUXIN UP RNA genes promote cell expansion. *Plant J.* 70: 978–990.

Spartz, A.K., Ren, H., Park, M.Y., Grandt, K.N., Lee, S.H., Murphy, A.S., et al. (2014) SAUR inhibition of PP2C-D phosphatases activates plasma membrane H^+-ATPases to promote cell expansion in *Arabidopsis*. *Plant Cell* 26: 2129–2142.

Sweetlove, L.J., Beard, K.F.M., Nunes-Nesi, A., Fernie, A.R. and Ratcliffe, R.G. (2010) Not just a circle: flux modes in the plant TCA cycle. *Trends Plant Sci.* 15: 462–470.

Szecowka, M., Heise, R., Tohge, T., Nunes-Nesi, A., Vosloh, D., Huege, J., et al. (2013) Metabolic fluxes in an illuminated *Arabidopsis* rosette. *Plant Cell* 25: 694–714.

Takahashi, K., Hayashi, K. and Kinoshita, T. (2012) Auxin activates the plasma membrane H^+-ATPase by phosphorylation during hypocotyl elongation in *Arabidopsis*. *Plant Physiol.* 159: 632–641.

Tong, Y., Zhou, J.J., Li, Z. and Miller, A.J. (2005) A two-component high-affinity nitrate uptake system in barley. *Plant J.* 41: 442–450.

Tränkner, M., Tavakol, E. and Jákli, B. (2018) Functioning of potassium and magnesium in photosynthesis, photosynthate translocation and photoprotection. *Physiol. Plant.* 163: 414–431.

Wong, J.H., Klejchová, M., Snipes, S.A., Nagpal, P., Bak, G., Wang, B., et al. (2021) SAUR proteins and PP2C.D phosphatases regulate H^+-ATPases and K^+ channels to control stomatal movements. *Plant Physiol.* 185: 256–273.

Wong, J.H., Spartz, A.K., Park, M.Y., Du, M. and Gray, W.M. (2019) Mutation of a conserved motif of PP2C.D phosphatases confers SAUR immunity and constitutive activity. *Plant Physiol.* 181: 353–366.

Xiong, Y., McCormack, M., Li, L., Hall, Q., Xiang, C. and Sheen, J. (2013) Glucose-TOR signalling reprograms the transcriptome and activates meristems. *Nature* 496: 181–186.

Yoo, S.D., Cho, Y.H. and Sheen, J. (2007) Arabidopsis mesophyll protoplasts: a versatile cell system for transient gene expression analysis. *Nature Protoc.* 2: 1565–1572.

Zhang, M., Wang, Y., Chen, X., Xu, F., Ding, M., Ye, W., et al. (2021a) Plasma membrane H^+-ATPase overexpression increases rice yield via simultaneous enhancement of nutrient uptake and photosynthesis. *Nature Commun.* 12: 735.

Zhang, Y., Giese, J., Kerbler, S.M., Siemiatkowska, B., Perez de Souza, L., Alpers, J., et al. (2021b) Two mitochondrial phosphatases, PP2c63 and Sal2, are required for posttranslational regulation of the TCA cycle in *Arabidopsis*. *Mol. Plant* 14: 1104–1118.